



# Adsorption of arsenic (V) on magnetite-enriched particles separated from the mill scale

Muhammad Kashif Shahid<sup>1</sup> · San Phearom<sup>2</sup> · Young-Gyun Choi<sup>2</sup>

Received: 31 May 2018 / Accepted: 14 January 2019 / Published online: 22 January 2019  
© Springer-Verlag GmbH Germany, part of Springer Nature 2019

## Abstract

The magnetite-enriched particles (MEP) were separated from the mill scale on low magnetic intensity ranging from 300 to 500 gauss. The characterization of the MEP was done with scanning electron microscopy (SEM), energy dispersive X-ray spectroscopy (EDS) and X-ray diffraction (XRD). The adsorption efficiency of MEP was investigated with batch tests and column operation. The maximum adsorption capacity was observed about 12.69 mg of arsenate on 1 g of adsorbent. Langmuir and Freundlich isotherm models were used to explain the experimental data and it was found that adsorption followed the Langmuir model more closely. Four columns were operated based on empty bed contact time (0.5 h and 1 h) and particle size (75–150  $\mu\text{m}$  and 150–300  $\mu\text{m}$ ). The operated columns successfully removed arsenate from influent (0.5 mg/L concentration) during continuous operation for 6 weeks. This study introduces a cost effective and ecofriendly process for arsenate removal with MEP separated at low intensity of magnetic field.

**Keywords** Arsenate · Adsorption · Kinetics · Magnetite · Mill scale

## Introduction

Arsenic is a toxic and carcinogenic element that can cause severe environmental and health issues (Dubey et al. 2012; Chakraborti et al. 2016; Chen et al. 2017). It can be found in mineral forms due to its complexation with other atoms. On the basis of oxidation state, arsenite (+3) and arsenate (+5) are two fundamental forms of arsenic. Its existence in soil can alter the water quality. Beside other trace elements and metalloids, it is relatively moveable in the ecosystem. The

geochemical reactions and weathering of minerals (having arsenic) are the main reasons of dissolved arsenic in groundwater. The arsenic mobilization in oxidizing environment is one of the majors problems (Smedley et al. 2002; Iskandar et al. 2012; Sun et al. 2016). The toxic impact of arsenate on ecosystem and health has been addressed in many studies (Smith et al. 2006; Sarkar et al. 2008; Sarkar and Paul 2016; Marchant et al. 2017; Bassil et al. 2018).

World Health Organization (WHO) has specified the acceptance limit of arsenic at 0.01 mg/L (10 ppb). Beside WHO standards, some countries also have their own standard limits for arsenic in groundwater. The localities with high concentration of arsenic in groundwater need some treatment for reducing the arsenic concentration at recommended limit. The common techniques for arsenic remediation include coagulation–filtration–precipitation, membrane technology, ion exchange and adsorption (Zhang et al. 2012; Chatterjee and De 2017; Mohamed et al. 2017; Molinari and Argurio 2017). Among these methods, adsorption is mostly favored due to its low cost, simple and eco-friendly operation (McDonald et al. 2015; Lata and Samadder 2016). So many metal oxides have been introduced for adsorptive removal of arsenate and arsenite from contaminated water (Mohan and Pittman 2007).

---

This article is a part of Topical Collection in Environmental Earth Sciences on Water Sustainability: A Spectrum of Innovative Technology and Remediation Methods, edited by Dr. Derek Kim, Dr. Kwang-Ho Choo, and Dr. Jeongwan Kim.

---

**Electronic supplementary material** The online version of this article (<https://doi.org/10.1007/s12665-019-8066-x>) contains supplementary material, which is available to authorized users.

---

✉ Young-Gyun Choi  
youngchoi@cnu.ac.kr

<sup>1</sup> Department of Environmental and Chemical Convergence Engineering, Daegu University, Daegudae-ro 201, Jillyang, Gyeongsan, Gyeongbuk, Republic of Korea

<sup>2</sup> Department of Environmental Engineering, Chungnam National University, Daejeon, Republic of Korea

Among other adsorbents, iron oxides, especially magnetite has been applied for arsenic removal due to its higher surface area, micro/mesoporous morphology and reasonable adsorption capacity (Aredes et al. 2012). Arsenic adsorption on magnetite particles mainly depends on solution pH (Shipley et al. 2009, 2010; Farrell et al. 2014).

This study introduces a novel method for arsenate adsorption on magnetite-rich particles (MEP) separated from mill scale at low magnetic intensity. Mill scale constitutes wustite (FeO), hematite ( $\alpha$ -Fe<sub>2</sub>O<sub>3</sub>), magnetite (Fe<sub>3</sub>O<sub>4</sub>), elemental iron and small amount of oil and grease (Yavuz et al. 2009; de Buzin et al. 2014). The effectiveness of MEP was assessed with the batch experiments and column operation. Based on experimental data, we proposed a cost effective and ecofriendly process for separation of MEP from mill scale and their application for arsenate adsorption.

## Materials and methods

### Separation of MEP from the mill scale

The mill scale was obtained from a steel factory based in Korea. It forms on the surface of sheets or plates during their production by rolling red-hot iron. It has a plate-like structure with <20 mm diameter. It constitutes different iron oxides, elemental iron and varying oil and grease substances. The oil and grease contents were removed in pretreatment.

The operational scheme for separation of MEP is presented in Fig. 1. As the mill scale is a by-product of hot rolling of steel, it carries various impurities including oil and grease. The impurities were removed by alkali cleaning. 10 L of 0.1 N NaOH solution was used to wash 1 kg mill scale. Later it was rinsed with deionized (DI) water and dried at 70 °C for 24 h. The mill scale was ground in Ball mill system for 3 h to reduce the particle size. The obtained homogeneous powdered mill scale was dried for 24 h and sieved with different size standard meshes. MEP have a size range of 45–300  $\mu$ m. As the magnetite is a strong magnetic particle, it can be easily separated from mill scale at low magnetic intensity. However, the weak magnetic particles (paramagnetic particles) need a higher magnetic intensity for separation. The MEP strongly attracted by magnetic field and hence, these are separated from the diamagnetic particles with varying the intensity of magnetic field.

### Instrumental analysis and reagents

All the batch experiments were conducted at 250 rpm in the Jar Tester (J-USRC, Jisico, Japan). The pH of the solutions was measured with 96 pH-L2 (samsan) and the analytical thermometer was used to measure the temperature. The characterization of the MEP was done with powder X-ray

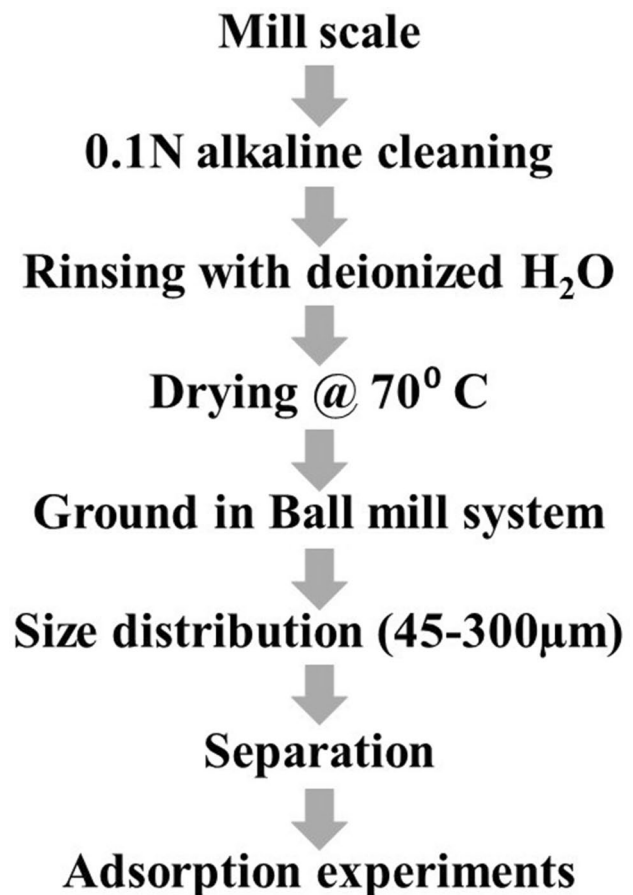


**Fig. 1** Operational scheme for the separation of magnetite-enriched particles from mill scale

diffraction (XRD) using Cu K $\alpha$  ( $\lambda = 1.5406 \text{ \AA}$ ) radiations, operated at 40 kV and 100 mA on Rigaku D/MAX-2500/PC (Rigaku Corp. Japan). Surface examination of the MEP was done with Hitachi SU-70 field emission scanning electron micrograph (SEM) and the elemental composition was identified with energy dispersive X-ray spectroscopy (EDS). Inductively coupled plasma mass spectroscopy (iCAP Q ICP-MS) manufactured by Thermo Scientific was used to analyze the arsenate concentration.

The analytical grade chemicals and reagents were used for all the experiments. Hydrochloric acid (HCl), sodium hydroxide (NaOH) and sulfuric acid (H<sub>2</sub>SO<sub>4</sub>) were obtained from Fisher scientific. Disodium hydrogen arsenate heptahydrate (sodium arsenate, dibasic) Na<sub>2</sub>HAsO<sub>4</sub>·7H<sub>2</sub>O (MW = 312.01) was used to prepare arsenate solution.

### Batch adsorption experiments

Batch experiments were done for the adsorption of arsenate on the MEP separated at low magnetic intensity (300–500 gauss) with 45–75  $\mu$ m size. The effect of initial

arsenate concentration on adsorption by MEP was examined by adding 1 g of MEP in to 1 L arsenate solution of different initial concentrations, i.e., 1, 5, 10, 20, 30 and 50 mg/L. The solutions were stirred at 250 rpm for 24 h. Temperature was controlled at 20 °C and the pH of the solution was adjusted at 6.5 with 0.1 N NaOH and 0.1 N HCl. Samples were collected and filtered prior to the analysis of arsenate concentration with ICP-MS system. The specific amount of absorbed arsenate on the MEP was calculated by the following equation,

$$q_e = \frac{C_i - C_e}{m} V \quad (1)$$

$$\% \text{Removal} = \frac{C_i - C_e}{C_i} (100) \quad (2)$$

here,  $q_e$  is the adsorption capacity (mg/g) at equilibrium,  $C_i$  and  $C_e$  are the initial and equilibrium concentrations of arsenate (mg/L), respectively,  $V$  is the volume (mL) of the aqueous solutions, and  $m$  is the mass (g) of adsorbent used in the experiments.

Langmuir and Freundlich isotherm models were used to describe the adsorption behavior. Both models are given below.

#### a. Langmuir model

$$\frac{C_e}{q_e} = \frac{1}{q_{\max} K_L} + \frac{C_e}{q_{\max}} \quad (3)$$

#### b. Freundlich model

$$\ln q_e = \frac{1}{n} \ln C_e + \ln K_F \quad (4)$$

where,  $q_{\max}$  is the maximum adsorption capacity (mg/g),  $K_L$  is the Langmuir constant (L/mg) while  $1/n$  and  $K_F$  are the Freundlich constants.

The kinetic study was carried out with 0.5 mg/L initial concentration of arsenate and 1 g/L magnetite-enriched particles. pH and temperature were also controlled at 6.5 and 20 °C, respectively. The mixture was stirred (250 rpm) for 2 h and the samples were collected 13 times (sampling interval is 1–30 min) after startup. The operational conditions were optimized according to the groundwater conditions and the earlier studies in the field (Giménez et al. 2007; Shahid et al. 2018).

The influence of pH on the arsenate adsorption was investigated by changing pH of the arsenate solutions of 10 mg/L concentration. The pH of the solutions was maintained at 2, 3, 4, 5, 6, 7, 8, 9, and 10 by adding either 0.1 N NaOH or 0.1 N HCl. The MEP (1 g/L) were added to the solutions

and the mixtures were stirred (250 rpm) at 20 °C for 4 h. Later the samples were collected and filtered before analysis of ionic concentration. To understand the effect of ionic strength of coexisting ions on arsenate removal, the ionic strength of the solutions was adjusted by adding NaCl to make the final concentrations of NaCl at 0.01, 0.1, and 1 M in the solution.

## Column operation

Column adsorption tests were performed using 4 sets of packed-bed columns. The inner diameter of the column was 3.5 cm, height was 40 cm and the volume was 384.85 cm<sup>3</sup>. The top and bottom chamber of the column were packed with glass beads having different size (1 and 10 mm in diameter) whereas the middle two portions (with 20 cm height) were packed with MEP, with a packing volume of 192.45 cm<sup>3</sup> (550 g). For the prevention of particle leaching from the middle portion of the column, a magnetic bar with screen was located. Four columns were operated with different particle sizes and empty bed contact time (EBCT) (Fig. 2; Table 1). A synthetic solution of arsenate with 0.5 mg/L concentration was used as an influent and prior to pump in the column, an influent pH was adjusted at 6.5. The presented data is obtained from first 63 days of column operation.

## Regeneration of columns after operation

MEP packed columns were regenerated with 0.2 N NaOH for 24 h with the flow rate of 1 mL/min. The arsenate concentration in an effluent was analyzed to know the leached amount of arsenate. The MEP packed column was thoroughly rinsed with deionized water after regeneration with alkali solution.

## Results and discussion

### Characterization of magnetite-enriched particles

Mill scale with size range 45–300 μm was used for the separation of strong magnetic particles from weak magnetic particles. Considering the mass fraction of mill scale, about 50% of particles were separated at low magnetic intensity. An earlier study discussed 38% magnetic fraction of mill scale as an equivalent of magnetite present in it (Martín et al. 2012). Over separated particles were found to have 80–85% mass fraction of magnetite and the remaining part consisted of wustite and hematite. Hence, the particles separated at low magnetic intensity were found to constitute mainly the magnetite. The XRD pattern of separated particles is presented in Fig. 3. The obtained



**Fig. 2** Photo of the column operation with column design parameters at right side

**Table 1** Description of column operation

Column	Magnetite-enriched particle size ( $\mu\text{m}$ )	EBCT (h)	Flow rate (mL/min)
C1	75–150	0.5	6.41
C2	150–300	0.5	6.41
C3	75–150	1	3.205
C4	150–300	1	3.205

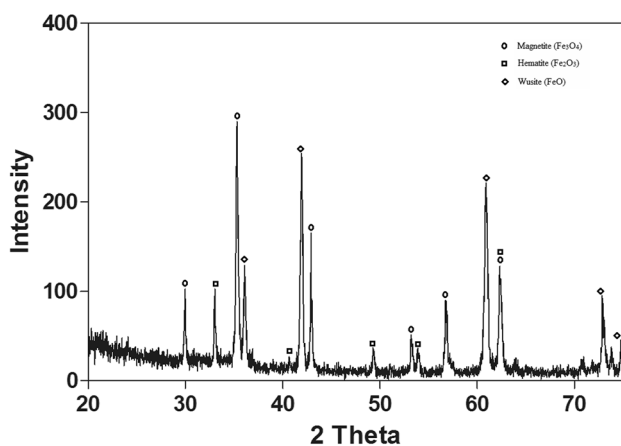


**Fig. 3** XRD pattern of separated particles

XRD pattern was found very close to the standard pattern (JCPDS 19–0629) of magnetite. However, some additional peaks were also observed for wustite and hematite, which were found to constitute 10–15% of separated particles. Hence, the term MEP was coined for separated particles in this study. The observed XRD pattern was found in consistency with previous studies on mill scale derived ferrite

particles (Yean et al. 2005; de Buzin et al. 2014; Shahid et al. 2018).

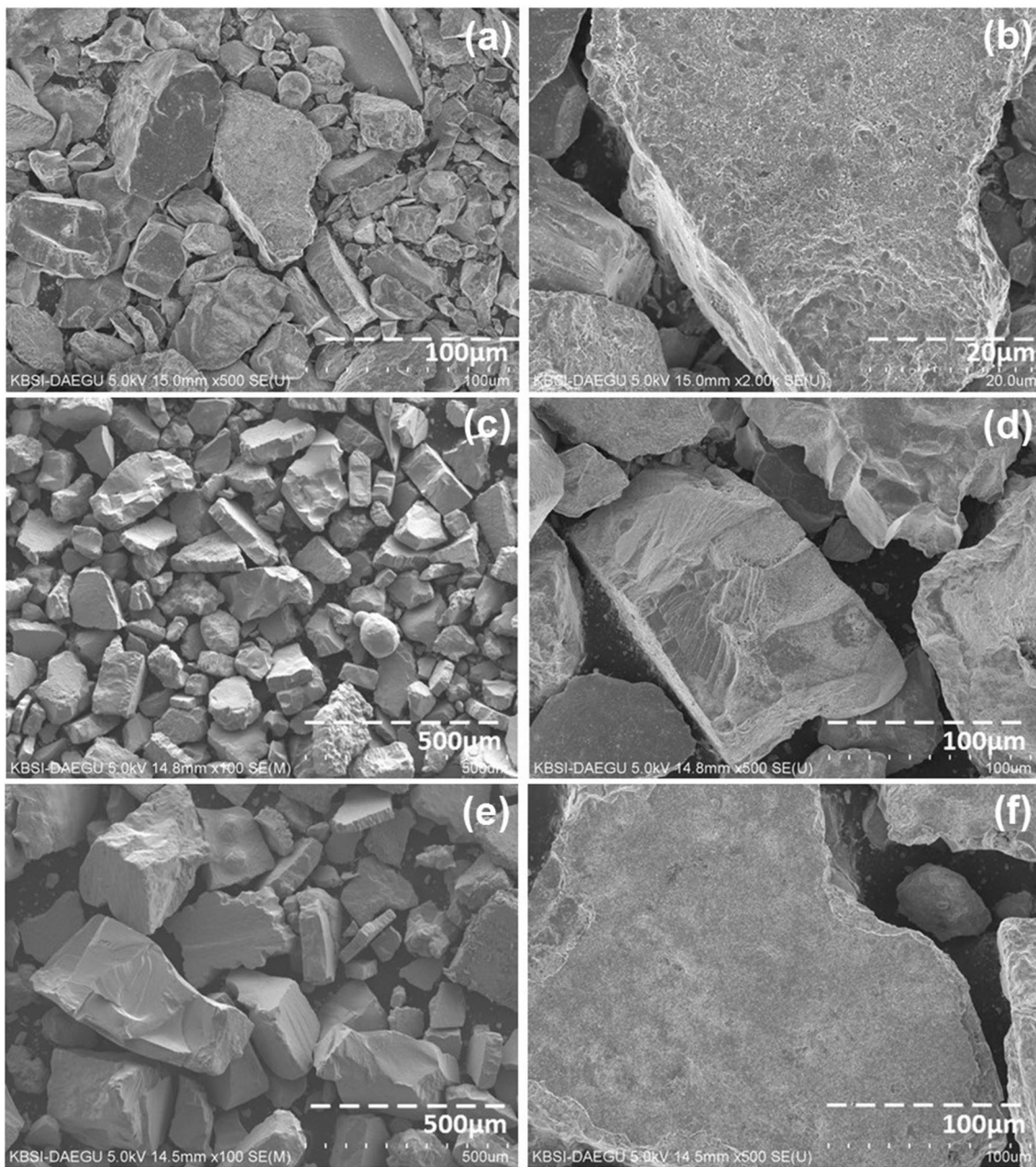
The morphological structure and the elemental composition of the separated particles examined with SEM and EDS analysis. SEM images of the separated particles indicated an asymmetrical shape and wide-ranging size, i.e., from less than 1  $\mu\text{m}$  to more than 300  $\mu\text{m}$  (Fig. 4). It seems that the van der Waals forces and the magneto-dipole attraction resulted in gathering of small particles led by irregular shape and size. The observed structure of particles was found similar to other studies (Potapova et al. 2012; Salazar-Camacho et al. 2013). At 500 nm scale (Fig. S1), SEM images indicated the agglomerate porous structure of separated particles which was also agreed by an earlier study (Legodi and de Waal 2006).

Figure 5 shows the EDS spectra for the separated particles of different size distributions. Oxygen and iron were identified as the main constituents of MEP. The higher atomic share of oxygen was found as compared with iron (Table 2). The higher atomic share of oxygen means an increase in possible adsorption localities. The high atomic share of oxygen indicates the possibility of large number of adsorption sites. The mechanism of arsenate adsorption on separated particles is supposed to be similar with adsorption mechanism of magnetite particles which is well described in previous studies (Liu et al. 2015; Freitas et al. 2016; Han et al. 2016). No other element was identified by EDS, which shows that impurities, if any, were successfully removed during pre-treatment and separation.

### Adsorption isotherm

Figure 6 shows the adsorption isotherm for the MEP. The initial arsenate concentration in the solution varied from 1





**Fig. 4** SEM micrograph of separated particles with wide range of size, i.e., 45–75  $\mu\text{m}$  (a, b), 75–150  $\mu\text{m}$  (c, d) and 150–300  $\mu\text{m}$  (e, f)

to 50 mg/L and the amount of MEP was kept 1 g/L. About 80% of the arsenate concentration was adsorbed on 1 g of MEP from the solution having 1 mg/L initial concentration. It was observed that by increasing the initial arsenate concentration, adsorption capacity starts to decrease. About 25% of arsenate from the higher concentration (50 mg/L) of the arsenate was adsorbed on 1 g of MEP. For the solution having 50 mg/L initial concentration, the maximum adsorption quantity was 12.69 of arsenate on 1 g of MEP. The quick adsorption was observed for all the solutions at the beginning of experiments. This happened

due to the maximum available sites for adsorption. As the arsenate concentration in the solution decreases, the rate of diffusion also decreases. After a certain time, no diffusion happened and the system reached the equilibrium state. The solutions having low arsenate concentration achieved equilibrium state much faster as compared with the solutions having higher concentration of arsenate. Followed by fulfillment of all the adsorption sites, the surface precipitation can also be progressed (Aredes et al. 2012). The parameters of Langmuir and Freundlich isotherms are given in Table 3. The higher value of correlation

**Fig. 5** EDS spectra of separated particles with wide range of size, i.e., 45–75  $\mu\text{m}$  (a), 75–150  $\mu\text{m}$  (b) and 150–300  $\mu\text{m}$  (c)

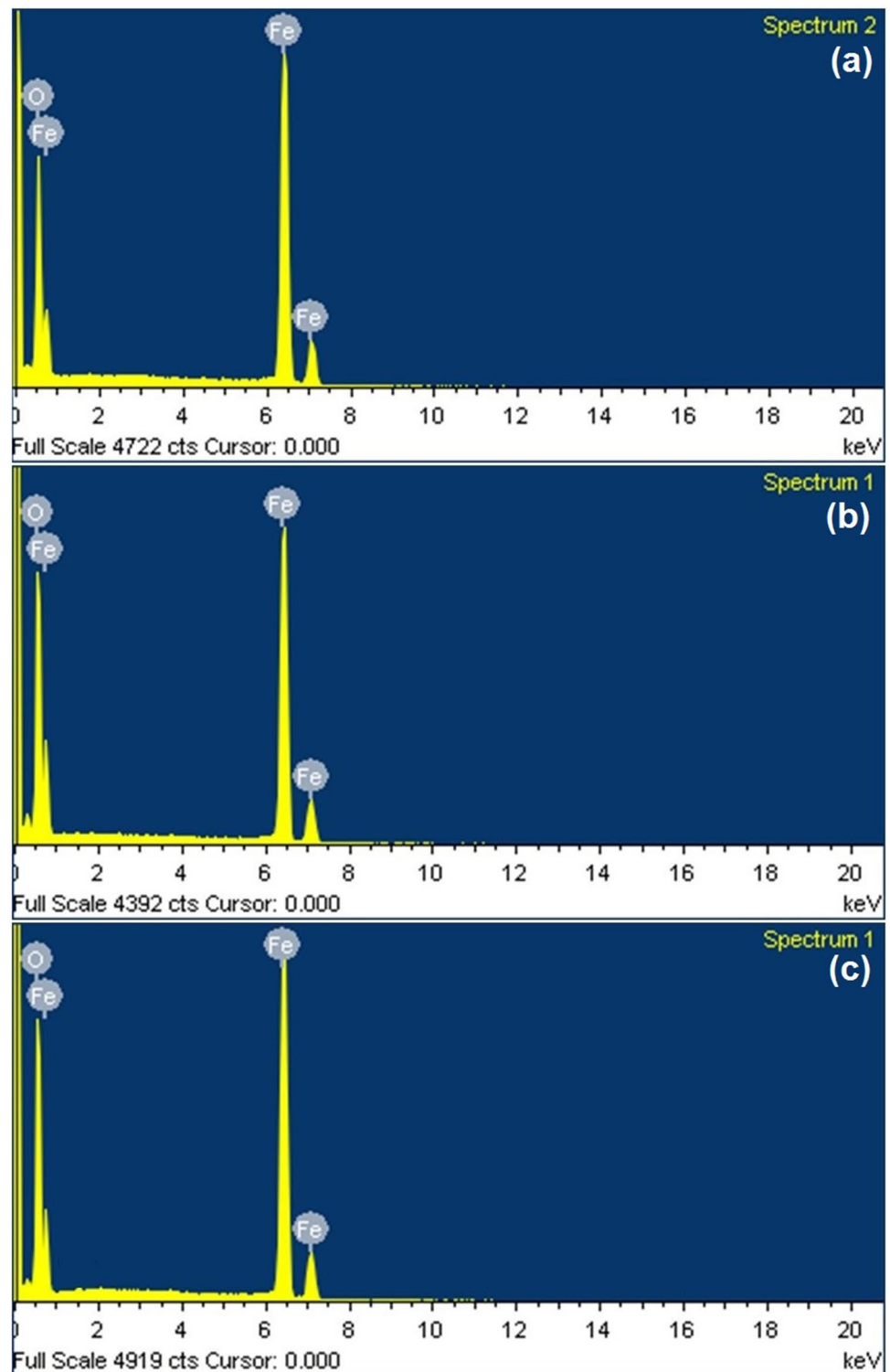
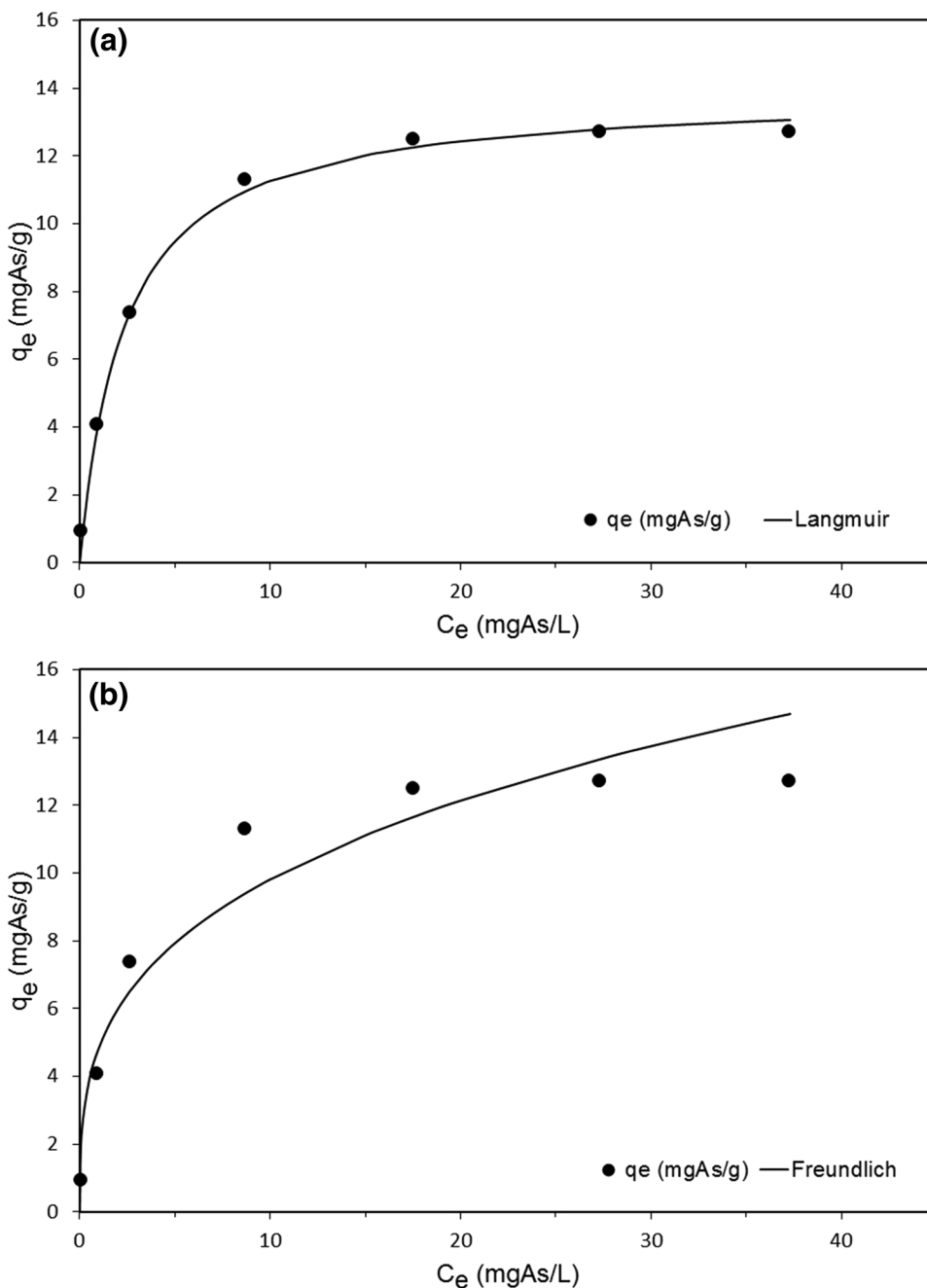


**Table 2** Elemental composition of MEP

Element	45–75 $\mu\text{m}$	75–150 $\mu\text{m}$	150–300 $\mu\text{m}$
O	54.7	60.07	59.25
Fe	45.3	39.93	40.75

coefficient ( $R^2$ ) for Langmuir (0.99) as compared with Freundlich (0.90) shows that the arsenate adsorption on magnetite-rich particles followed Langmuir model more closely. It indicates that most of the adsorption occurred on the surface layer of adsorbent (Keyhanian et al. 2016).

**Fig. 6** Adsorption isotherm of MEP



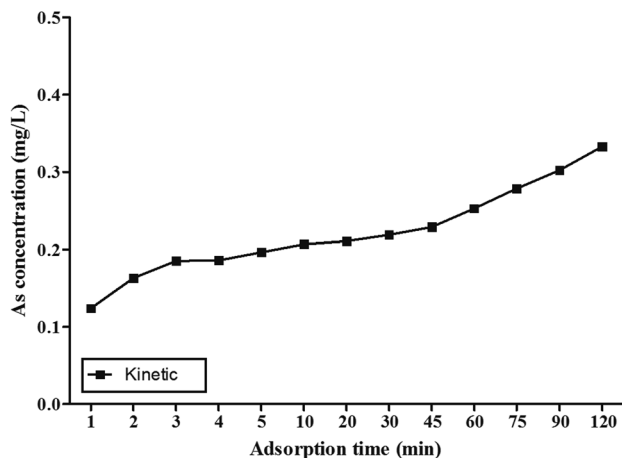
**Adsorption kinetic**

Figure 7 shows the effect of contact time on the adsorption of arsenate on MEP. The experiment was conducted for 2 h with 0.5 mg/L initial concentration of arsenate. About 0.12 mg concentration of arsenate was adsorbed on MEP after 1 min contact time. However, maximum 0.32 mg of arsenate was adsorbed on 1 g of MEP at the end of 2 h experiment. It seems that the speedy adsorption happened at the start of the experiment, and later, the system attained an equilibrium state. Initially, all accessible

adsorption locations were occupied by arsenate. Later, the arsenate diffused through the interior pores of the magnetite-enriched particles and hence, the reaction adsorption kinetics is directed by this arsenate diffusion. The diffusion rate depends on the concentration of arsenate in the solution. As the concentration of arsenate decreases in the solution, the diffusion rate also decreases and at the end no further diffusion takes place and hence, adsorption reaction attains the equilibrium state. At the low surface coverage conditions, arsenic favored the monodentate complex formation while it forms bidentate mononuclear complex at high surface

**Table 3** Estimated values of various parameters of Langmuir and Freundlich models for the removal of arsenate by MEP

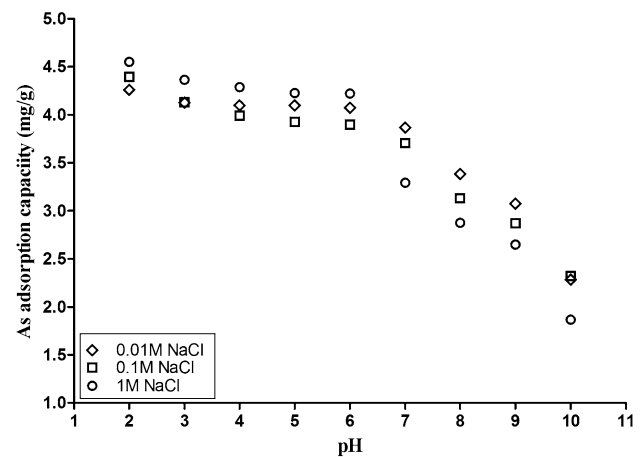
Isotherm model	
Langmuir parameters	
$q_{\max}$	13.88 mg/g
$K_L$	0.432
$R^2$	0.99
Freundlich parameters	
$K_F$	4.851 mg/g
$1/n$	0.3065
$R^2$	0.90

**Fig. 7** Kinetic of MEP separated at 500 gauss

coverage. The monodentate complex forms rapidly as compared with bidentate complex formation (Raven et al. 1998).

### Effect of pH and ionic strength

Figure 8 shows the effect of pH and the ionic strength of coexisting ions on the adsorption of arsenate on MEP. The initial arsenate concentration in a solution was maintained at 10 mg/L and 1 g/L of MEP was used. The acidic condition seems an ideal state for arsenate adsorption on MEP. The adsorption was relatively stable at pH 6. An increase in pH caused serious decline in adsorption curve. The net surface charge on MEP remains negative at basic pH, which results in repulsion for neighboring arsenate anions. The surface charge of iron oxides remains negative at pH more than 6 and positive below than pH 6 (Legodi and de Waal 2006; Giraldo and Moreno-piraján 2013). Therefore, it can be stated that any variation in pH can leave a significant impact on the net surface charge of MEP, which may results in different adsorption behavior. Different molar concentrations of NaCl were introduced in

**Fig. 8** Effect of pH and ionic strength on arsenate adsorption by MEP

the arsenate solution but no specific change in adsorption was observed. It shows that in the presence of other ions, the arsenate adsorption behavior does not change for MEP.

### Column operation

Figure 9 shows the adsorption behavior of all columns with 0.5 mg/L initial arsenate concentration in an influent. The pH of an influent stream for all columns remained constant (6.5) during the entire operation (Fig. S2). The column operation indicated the successful removal of arsenate from contaminated water for more than 6 weeks. The columns were regenerated with alkaline solution after continuous operation for 48 days. The impact of influent flow rate on arsenate adsorption by MEP was investigated by changing the flow rate from 3.2 (1 h EBCT) to 6.4 mL/min (0.5 h EBCT) and keeping the adsorbent dose (550 g), initial arsenic concentration (0.5 mg/L) and pH (6.5) constant. The breakthrough curves indicated that an increase in flow rate causes decrease in adsorption capacity. This phenomenon can be described based on less contact time between arsenate solution and adsorbent packed column. This less contact time results in the low adsorption of arsenate on the surface of MEP. The entire operation indicated that a column packed with MEP can be operated efficiently for 6 weeks without regeneration and 0.5 mg/L concentration of arsenate can easily be removed. No blockage was observed in operated columns during the entire operation and hence, an effluent flow rate did not specify any drastic change (Fig. S3). Finally, based on column operation and daily adsorptive amount of arsenate on MEP (Fig. S4), it can be concluded that up to 0.5 mg/L initial arsenate concentration of solution can effectively remove in continuous operation for 3 and 5 weeks with 0.5 and 1 h EBCT, respectively.



**Fig. 9** The operational behavior of columns

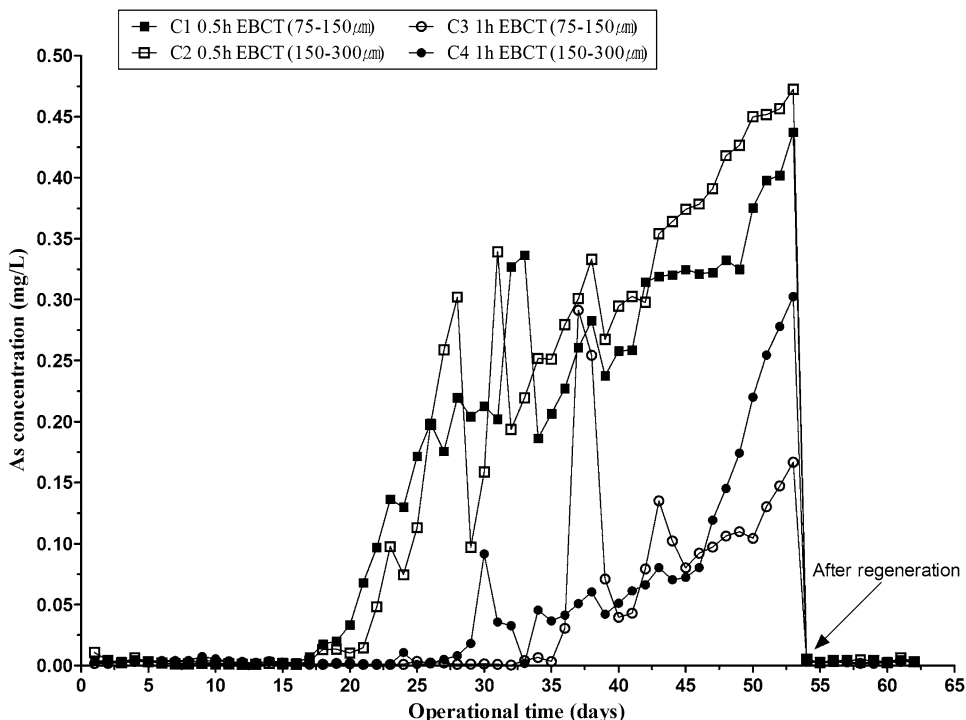


**Table 4** Adsorptive and leached amount of arsenate from columns packed with MEP

Column	Dosage	Absorbed	Leached	
EBCT 0.5 h	C1 (75–150 μm)	244.535	86.218	83.697
	C2 (150–300 μm)		83.458	70.653
EBCT 1 h	C3 (75–150 μm)	122.267	64.850	57.746
	C4 (150–300 μm)		63.730	60.628

**Regeneration**

Columns were regenerated with alkaline solution and the leached amount of arsenate was recorded. The comparison between adsorptive and leached amount of arsenate during column operation is presented in Table 4. It was observed that alkali cleaning can successfully remove over 90% of adsorbed arsenate from the surface of magnetite-enriched particles.

**Conclusions**

This study discusses the separation of MEP from the mill scale and its application for the adsorption of arsenate. MEP were successfully separated at low intensity of magnetic field and characterized with XRD, SEM and EDS. The adsorption efficiency of MEP was examined with batch experiments and column operation. The maximum adsorption

quantity was found about 12.69 of arsenate on 1 g of MEP. The obtained data was plotted in Langmuir and Freundlich isotherm models, which indicates that the data more closely fit in Langmuir model. Hence, it was assumed that most of the arsenate was adsorbed at the first layer of MEP. Four columns were operated with different EBCT and particle size and the successful adsorption of arsenate was observed for 6 weeks. The operational behavior of column showed that an increase in flow rate cause decrease in adsorption capacity. The main reason behind this phenomenon is a less contact time between arsenate solution and MEP. However, in case 0.5 mg/L initial arsenate concentration, the column operation was found successful to remove all of arsenate concentration for 3 and 5 weeks with 0.5 and 1 h EBCT, respectively. The columns were regenerated after 48 days operation and the sorption capacity of MEP was reinstated at initial condition. Finally, it can be stated that low-cost MEP can be separated and used for adsorption of arsenate.

**Acknowledgements** This work was supported by “Development of Eco-Smart Waterworks System” Program by the Ministry of Environment (MOE), Republic of Korea (Project #: 2016002110009).

**References**

Aredes S, Klein B, Pawlik M (2012) The removal of arsenic from water using natural iron oxide minerals. *J Clean Prod* 29–30:208–213. <https://doi.org/10.1016/j.jclepro.2012.01.029>

- Bassil M, Daou F, Hassan H et al (2018) Lead, cadmium and arsenic in human milk and their socio-demographic and lifestyle determinants in Lebanon. *Chemosphere* 191:911–921. <https://doi.org/10.1016/j.chemosphere.2017.10.111>
- Chakraborti D, Rahman MM, Ahamed S et al (2016) Arsenic groundwater contamination and its health effects in Patna district (capital of Bihar) in the middle Ganga plain, India. *Chemosphere* 152:520–529. <https://doi.org/10.1016/j.chemosphere.2016.02.119>
- Chatterjee S, De S (2017) Adsorptive removal of arsenic from groundwater using chemically treated iron ore slime incorporated mixed matrix hollow fiber membrane. *Sep Purif Technol* 179:357–368. <https://doi.org/10.1016/j.seppur.2017.02.019>
- Chen J, Qian H, Wu H et al (2017) Assessment of arsenic and fluoride pollution in groundwater in Dawukou area, Northwest China, and the associated health risk for inhabitants. *Environ Earth Sci* 76:1–15. <https://doi.org/10.1007/s12665-017-6629-2>
- de Buzin PGWK, Vigânico EM, Silva RDA et al (2014) Production of ferrous sulfate from steelmaking mill scale. *Int J Sci Eng Res* 5:353–359
- Dubey CS, Mishra BK, Shukla DP et al (2012) Anthropogenic arsenic menace in Delhi Yamuna flood plains. *Environ Earth Sci* 65:131–139. <https://doi.org/10.1007/s12665-011-1072-2>
- Farrell JW, Fortner J, Work S et al (2014) Arsenic removal by nanoscale magnetite in Guanajuato, Mexico. *Environ Eng Sci* 31:393–402. <https://doi.org/10.1089/ees.2013.0425>
- Freitas ETF, Stroppa DG, Montoro LA et al (2016) Arsenic entrapment by nanocrystals of Al-magnetite: the role of Al in crystal growth and As retention. *Chemosphere* 158:91–99. <https://doi.org/10.1016/j.chemosphere.2016.05.044>
- Giménez J, Martínez M, de Pablo J et al (2007) Arsenic sorption onto natural hematite, magnetite, and goethite. *J Hazard Mater* 141:575–580. <https://doi.org/10.1016/j.jhazmat.2006.07.020>
- Giraldo L, Moreno-piraján JC (2013) Synthesis of magnetite nanoparticles and exploring their application in the removal of Pt<sup>2+</sup> and Au<sup>3+</sup> ions from aqueous solutions. *Eur Chem Bull* 2:445–452. <https://doi.org/10.17628/ecb.2013.2.445-452>
- Han X, Song J, Li YL et al (2016) As(III) removal and speciation of Fe (oxyhydr)oxides during simultaneous oxidation of As(III) and Fe(II). *Chemosphere* 147:337–344. <https://doi.org/10.1016/j.chemosphere.2015.12.128>
- Iskandar I, Koike K, Sendjaja P (2012) Identifying groundwater arsenic contamination mechanisms in relation to arsenic concentrations in water and host rocks. *Environ Earth Sci* 65:2015–2026. <https://doi.org/10.1007/s12665-011-1182-x>
- Keyhanian F, Shariati S, Faraji M, Hesabi M (2016) Magnetite nanoparticles with surface modification for removal of methyl violet from aqueous solutions. *Arab J Chem* 9:S348–S354. <https://doi.org/10.1016/j.arabjc.2011.04.012>
- Lata S, Samadder SR (2016) Removal of arsenic from water using nano adsorbents and challenges: a review. *J Environ Manag* 166:387–406. <https://doi.org/10.1016/j.jenvman.2015.10.039>
- Legodi MA, de Waal D (2006) The preparation of magnetite, goethite, hematite and maghemite of pigment quality from mill scale iron waste. *Dye Pigment* 74:161–168. <https://doi.org/10.1016/j.dyepig.2006.01.038>
- Liu C, Chuang Y, Chen T et al (2015) Mechanism of arsenic adsorption on magnetite nanoparticles from water: thermodynamic and spectroscopic studies. *Environ Sci Technol* 49:7726–7734. <https://doi.org/10.1021/acs.est.5b00381>
- Marchant BP, Saby NPA, Arrouays D (2017) A survey of topsoil arsenic and mercury concentrations across France. *Chemosphere* 181:635–644. <https://doi.org/10.1016/j.chemosphere.2017.04.106>
- Martín MI, López FA, Torralba JM (2012) Production of sponge iron powder by reduction of rolling mill scale. *Ironmak Steelmak* 39:155–162. <https://doi.org/10.1179/1743281211Y.0000000078>
- McDonald KJ, Reddy KJ, Singh N et al (2015) Removal of arsenic from groundwater in West Bengal, India using CuO nanoparticle adsorbent. *Environ Earth Sci* 73:3593–3601. <https://doi.org/10.1007/s12665-014-3645-3>
- Mohamed A, Osman TA, Toprak MS et al (2017) Surface functionalized composite nanofibers for efficient removal of arsenic from aqueous solutions. *Chemosphere* 180:108–116. <https://doi.org/10.1016/j.chemosphere.2017.04.011>
- Mohan D, Pittman CU (2007) Arsenic removal from water/wastewater using adsorbents—a critical review. *J Hazard Mater* 142:1–53. <https://doi.org/10.1016/j.jhazmat.2007.01.006>
- Molinari R, Argurio P (2017) Arsenic removal from water by coupling photocatalysis and complexation–ultrafiltration processes: a preliminary study. *Water Res* 109:327–336. <https://doi.org/10.1016/j.watres.2016.11.054>
- Potapova E, Yang X, Westerstrand M et al (2012) Interfacial properties of natural magnetite particles compared with their synthetic analogue. *Miner Eng* 36–38:187–194. <https://doi.org/10.1016/j.mineng.2012.03.030>
- Raven KP, Jain A, Loeppert RH (1998) Arsenite and arsenate adsorption on ferrihydrite: kinetics, equilibrium, and adsorption envelopes. *Environ Sci Technol* 32:344–349. <https://doi.org/10.1021/es970421p>
- Salazar-Camacho C, Villalobos M, Luz Rivas-Sánchez M de la et al (2013) Characterization and surface reactivity of natural and synthetic magnetites. *Chem Geol* 347:233–245. <https://doi.org/10.1016/j.chemgeo.2013.03.017>
- Sarkar A, Paul B (2016) The global menace of arsenic and its conventional remediation—a critical review. *Chemosphere* 158:37–49. <https://doi.org/10.1016/j.chemosphere.2016.05.043>
- Sarkar S, Blaney LM, Gupta A et al (2008) Arsenic removal from groundwater and its safe containment in a rural environment: validation of a sustainable approach. *Environ Sci Technol* 42:4268–4273. <https://doi.org/10.1021/es702556t>
- Shahid MK, Phearom S, Choi Y-G (2018) Synthesis of magnetite from raw mill scale and its application for arsenate adsorption from contaminated water. *Chemosphere* 203:90–95. <https://doi.org/10.1016/j.chemosphere.2018.03.150>
- Shibley HJ, Yean S, Kan AT, Tomson MB (2009) Adsorption of arsenic to magnetite nanoparticles: effect of particle concentration, pH, ionic strength, and temperature. *Environ Toxicol Chem* 28:509–515. <https://doi.org/10.1897/08-155.1>
- Shibley HJ, Yean S, Kan AT, Tomson MB (2010) A sorption kinetics model for arsenic adsorption to magnetite nanoparticles. *Environ Sci Pollut Res* 17:1053–1062. <https://doi.org/10.1007/s11356-009-0259-5>
- Smedley PL, Nicolli HB, Macdonald DMJ et al (2002) Hydrogeochemistry of arsenic and other inorganic constituents in groundwaters from La Pampa, Argentina. *Appl Geochem* 17:259–284. [https://doi.org/10.1016/S0883-2927\(01\)00082-8](https://doi.org/10.1016/S0883-2927(01)00082-8)
- Smith AH, Marshall G, Yuan Y et al (2006) Increased mortality from lung cancer and bronchiectasis in young adults after exposure to arsenic in utero and in early childhood. *Environ Health Perspect* 114:1293–1296. <https://doi.org/10.1289/ehp.8832>
- Sun J, Quicksall AN, Chillrud SN et al (2016) Arsenic mobilization from sediments in microcosms under sulfate reduction. *Chemosphere* 153:254–261. <https://doi.org/10.1016/j.chemosphere.2016.02.117>
- Yavuz CT, Prakash A, Mayo JT, Colvin VL (2009) Magnetic separations: from steel plants to biotechnology. *Chem Eng Sci* 64:2510–2521. <https://doi.org/10.1016/j.ces.2008.11.018>
- Yean S, Cong L, Yavuz CT et al (2005) Effect of magnetite particle size on adsorption and desorption of arsenite and

arsenate. *J Mater Res* 20:3255–3264. <https://doi.org/10.1557/jmr.2005.0403>

Zhang G, Li X, Wu S, Gu P (2012) Effect of source water quality on arsenic (V) removal from drinking water by coagulation/microfiltration. *Environ Earth Sci* 66:1269–1277. <https://doi.org/10.1007/s12665-012-1549-7>

**Publisher's Note** Springer Nature remains neutral with regard to jurisdictional claims in published maps and institutional affiliations.